Recognition of Guanine−Guanine Mismatches by the Dimeric Form of 2-Amino-1,8-naphthyridine

Kazuhiko Nakatani,*,† Shinsuke Sando,† Hiroyuki Kumasawa,† Jun Kikuchi,‡ and Isao Saito*,†

Contribution from the Department of Synthetic Chemistry and Biological Chemistry, Faculty of Engineering, Kyoto University, CREST, Japan Science and Technology Corporation (JST), Kyoto 606-8501, Japan, and Protein Research Group, Genomic Sciences Center (GSC), RIKEN, Yokohama Institute, Yokohama 230-0045, Japan

Received April 9, 2001

Abstract: Dimeric 2-amino-1,8-naphthyridine selectively binds to a G−G mismatch with high affinity (K_d = 53 nM). We have investigated a binding mechanism of naphthyridine dimer **2** to a G−G mismatch by spectroscopic studies, thermodynamic analysis, and structure−activity studies for the thermal stabilization of the mismatch. ^{1}H NMR spectra of a complex of **2** with 9-mer duplex d(CATCGGATG)$_2$ containing a G−G mismatch showed that all hydrogens in two naphthyridine rings of **2** were observed upfield compared to those of **2** in a free state. The 2D-NOESY experiments showed that each naphthyridine of **2** binds to a guanine in the G−G mismatch within the π-stack. In CD spectra, a large conformational change of the G−G mismatch-containing duplex was observed upon complex formation with **2**. Isothermal calorimetry titration of **2** binding to the G−G mismatch showed that the stoichiometry for the binding is about 1:1 and that the binding is enthalpy-controlled. It is clarified by structure−activity studies that show (i) the linker connecting two naphthyridine rings was essential for the stabilization of the G−G mismatch, (ii) the binding efficiency was very sensitive to the linker structure, and (iii) the binding of two naphthyridines to each one of two Gs in the G−G mismatch is essential for a strong stabilization. These results strongly supported the intercalation of both naphthyridine rings of **2** into DNA base pairs and the formation of a hydrogen bonded complex with the G−G mismatch.

Single nucleotide polymorphism (SNP) is a genetic difference of a single nucleotide base. SNP widely spreads over a whole genome sequence and exists in every 500−1000 base pairs. Since a draft sequence of human genome was determined,[1,2] SNP became extremely important as a genetic marker for the identification of disease genes and detection of genetic mutations.[3,4] Thus, simple and rapid detection of a single nucleotide difference in the DNA sequences is an indispensable technique for both SNP mapping and typing. A number of high throughput methods employing high-density arrays,[5,6] single-primer extension assays,[7] molecular beacons,[8] TaqMan PCR,[9] invader assays,[10] rolling-circle amplifications,[11] and MALDI-TOF mass spectrometry[12,13] have been developed for the detection of SNP. To distinguish a mutant DNA from its wild type, these methods for SNP detection require the sequence information, including the site of a mutation. Because both mutant and wild type DNAs are completely normal with respect to chemical structure and properties, it is very difficult to detect a single nucleotide difference of DNA sequences without knowing the sequence information. There is a way to transform structurally normal DNAs containing SNP into DNAs with structural defects. When two DNAs containing a single nucleotide difference were mixed, heat denatured, and annealed, a strand exchange between the mutant and wild-type DNAs occurred to produce the heteroduplexes containing a base mismatch in addition to regeneration of the original homoduplexes.[14] Mismatch-containing DNAs are considerably different from normal DNAs with respect to structure,[15−19] thermal stability,[20−23] binding to mismatch repair

* E-mail: nakatani@sbchem.kyoto-u.ac.jp.
† Faculty of Engineering, Kyoto University.
‡ Genomic Sciences Center, RIKEN.

(1) Lander, E. S. et al. *Nature* **2001**, *409*, 860−921.
(2) Venter, C. J. et al. *Science* **2001**, *291*, 1304−1351.
(3) Schafer, A. J.; Hawkins, J. R. *Nat. Biotechnol.* **1998**, *16*, 33−39.
(4) Collins, F. S.; Guyer, M. S.; Chakravarti, A. *Science* **1997**, *278*, 1580−1581.
(5) Wang, D. G.; Fan, J.-B.; Siao, C.-J.; Berno, A.; Young, P.; Sapolsky, R.; Ghandour, G.; Perkins, N.; Winchester, E.; Spencer, J.; Kruglyak, L.; Stein, L.; Hsie, L.; Topaloglou, T.; Hubbell, E.; Robinson, E.; Mittamann, M.; Morris, M. S.; Shen, N.; Kilburn, D.; Rioux, J.; Nusbaum, C.; Roen, S.; Hudson, T. J.; Lipshutz, R.; Chee, M.; Lander, E. S. *Science* **1998**, *280*, 1077−1082.
(6) For a review, see: Hacia, J. G. *Nat. Genet.* **1999**, *21*, 42−47 (supplement).
(7) Shumaker, J. M.; Metspalu, A.; Caskey, C. T. *Hum. Mutat.* **1996**, *7*, 346−354.
(8) Thagi, S.; Fratu, D. P.; Kramer, F. R. *Nat. Biotechnol.* **1998**, *16*, 49−53.
(9) Morris, T.; Robertson, B.; Gallagher, M. *J. Clin. Microbiol.* **1996**, *34*, 2933−2936.
(10) Lyamichev, V.; Mast, A. L.; Hall, J. G.; James R.; Prudent, J. R.; Kaiser, M. W.; Takova, T.; Robert, W.; Kwiatkowski, R. W.; Sander, T. J.; Arruda, M.; Arco, D. A.; Neri, B. P.; Brow, M. A. D. *Nat. Biotechnol.* **1999**, *17*, 292−296.
(11) Lizardi, P. M.; Huang, X.; Zhu, Z.; Bray-Ward, P.; Thomas, D. C.; Ward, D. C. *Nat. Genet.* **1998**, *19*, 225−232.
(12) Haff, L.; Smirnov, I. *Genome Res.* **1997**, *7*, 378−388.
(13) Ross, P.; Hall, L.; Smirnov, I.; Haff, L. *Nat. Biotechnol.* **1998**, *16*, 1347−1351.
(14) For a review of heteroduplex formation and analysis, see: Nataraj, A. J.; Olivos-Glander, I.; Kusukawa, N.; Highsmith, W. E., Jr. *Electrophoresis* **1999**, *20*, 1177−1185.
(15) Hunter, W. N.; Brown, T.; Kennard, O. *J. Biomol. Struct. Dyn.* **1986**, *4*, 173−191.

10.1021/ja0109186 CCC: $20.00 © 2001 American Chemical Society
Published on Web 11/22/2001

enzymes,[24,25] and susceptibility to drug interactions.[26−32] These physical and chemical properties characteristic of mismatches are the keys for the detection of heteroduplexes.

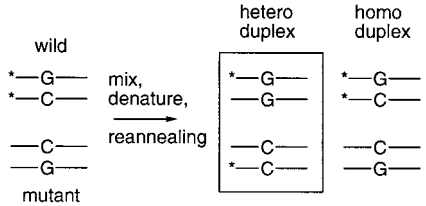

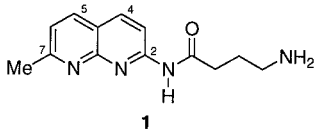

1

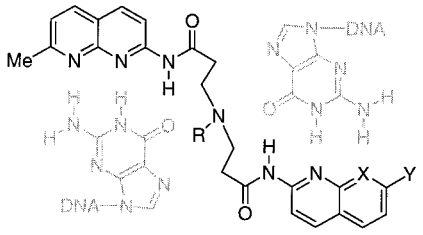

2 : R = H, X = N, Y = Me
3 : R = $CO(CH_2)_3NH_2$, X = N, Y = Me
4 : R = H, X = CH, Y = H

We have reported that 2-amino-1,8-naphthyridine derivative **1** possessing the hydrogen bonding groups fully complementary to guanine (G) binds selectively to a G bulge in duplex DNA.[33,34] We have rationalized that **1**binds to bulged G by forming three hydrogen bonds and the hydrogen-bonded pair of **1**−G is stabilized in the duplex by stacking with the immediate base pairs flanking the bulge. Because **1** binds to G but not to adenine (A), thymine (T), and cytosine (C) bulges, a formation of three hydrogen bonds between **1** and G effectively discriminates a G bulge from the others (Figure 1a). We have extended the hypothesis to the recognition of a G−G mismatch by assuming a G−G mismatched site as two consecutive G bulges. It has been known that G−G mismatches form a stable base pair in duplex DNA.[35−37] However, we anticipated that an interaction of 2-aminonaphthyridine to one of the Gs in the G−G mismatch may produce a pseudo G bulge as a hypothetical intermediate structure, which is subsequently bound by another molecule of naphthyridine forming two hydrogen-bonded pairs of G−naphthyridine in a duplex π-stack (Figure 1b).

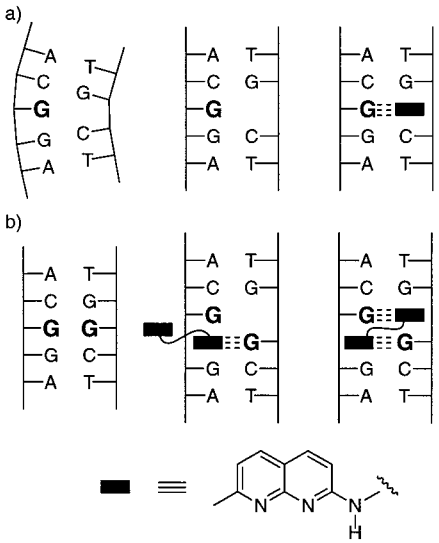

Figure 1. Illustrations of proposed schemes for G bulge and G−G mismatch recognition by **1** and its dimeric form, respectively. (a) G bulge changes its conformation so as to bind **1** opposite the bulge. A stacked-in conformation was shown as a representative of the initial structures of a G bulge. (b) G−G mismatch binds to one naphthyridine to produce a pseudo G bulge that allows the binding of another naphthyridine.

We have synthesized naphthyridine dimer **2** and investigate its binding to a G−G mismatch in duplex DNA.[38] DNase I footprint titration showed that **2** selectively and strongly binds to a G−G mismatch with the dissociation constant of 53 nM. The affinity of **2** to G−A and G−T mismatches is about 360-fold lower than that to a G−G mismatch. No apparent binding of **2** to normal DNA containing only Watson−Crick base pairs was observed. We have developed a mismatch-detecting sensor useful for a surface plasmon resonance (SPR) assay by immobilizing **2** onto the dextran-coated gold surface.[38] With this sensor, we have succeeded in differentiating 652 base pairs of PCR products of a G/C heterozygote from those of a G/G homozygote of HSP70-2 gene regarding the base at a nucleotide number of 2345.[39] For the accurate detection of SNP by mismatch-binding drugs, recognition of each one of eight mismatches by different drugs is ideal. Precise understanding of the mechanism for the G−G mismatch recognition by **2** would provide useful information for the molecular design of the drugs targeting other base mismatches. We herein report

(16) Webster, G. D.; Sanderson, M. R.; Skelly, J. V.; Swann, P. F.; Li, B. F.; Tickel, I. J. *Proc. Natl. Acad. Sci. U.S.A.* **1990**, *87*, 6693−6697.
(17) Gao, X.; Patel, D. J. *J. Am. Chem. Soc.* **1988**, *110*, 5178−5182.
(18) Nikonowicz, E. P.; Meadows, R. P.; Fagan, P.; Gorenstein, D. G. *Biochemistry* **1991**, *30*, 1323−1334.
(19) Allawi, H. T.; SantaLucia, J., Jr. *Biochemistry* **1997**, *36*, 10581−10594.
(20) Aboul-ela, F.; Koh, D.; Tinoco, I., Jr.; Martin, F. H. *Nucleic Acids Res.* **1985**, *13*, 4811−4824.
(21) Li, Y.; Zon, G.; Wilson, W. D. *Biochemistry* **1991**, *30*, 7566−7572.
(22) Li. Y.; Agrawal, S. *Biochemistry* **1995**, *34*, 10056−10062.
(23) Allawi, H. T.; SantaLucia, J., Jr. *Biochemistry* **1998**, *37*, 2170−2179.
(24) Fazakerley, G. V.; Qignard, E.; Woisard, A.; Guschlbauer, W.; van der Marel, G. A.; van Boom, J. H.; Jones, M.; Radman, M. *EMBO. J.* **1986**, *5*, 3697−3703.
(25) Smith, J.; Modrich, P. *Proc. Natl. Acad. Sci. U.S.A.* **1996**, *93*, 4374−4379.
(26) Kappen, L. S.; Goldberg, I. H. *Proc. Natl. Acad. Sci. U.S.A.* **1992**, *89*, 6706−6710.
(27) Kappen, L. S.; Goldberg, I. H. *Biochemistry* **1992**, *31*, 9081−9089.
(28) Chen, F.-U. *Biochemistry* **1998**, *37*, 3955−3964.
(29) Lee, S.-J.; Hurley, L. H. *J. Am. Chem. Soc.* **1999**, *121*, 8971−8977.
(30) Yang, X.-L.; Hubbard, R. B., IV; Lee, M.; Tao, Z.-F.; Sugiyama, H.; Wang, A. H. *Nucleic Acids Res.* **1999**, *27*, 4183−4190.
(31) Jackson, B. A.; Alekseyev, V. Y.; Barton, J. K. *Biochemistry* **1999**, *38*, 4655−4662.
(32) Jackson, B. A.; Barton, J. K. *Biochemistry* **2000**, *39*, 6176−6182.
(33) Nakatani, K.; Sando, S.; Saito, I. *J. Am. Chem. Soc.* **2000**, *122*, 2172−2177.
(34) Nakatani, K.; Sando, S.; Yoshida, K.; Saito, I. *Bioorg. Med. Chem. Lett.* **2001**, *11*, 335−337.
(35) Faibis, V.; Cognet, J. A.; Boulard, Y.; Sowers, L. C.; Fazakerley, G. V. *Biochemistry* **1996**, *35*, 14452−14464.
(36) Lane, A. N.; Peck, B. *Eur. J. Biochem.* **1995**, *230*, 1073−1087.
(37) Borden, K. L.; Jenkins, T. C.; Skelly, J. V.; Brown, T.; Lane, A. T. *Biochemistry* **1992**, *31*, 5411−5422.
(38) Nakatani, K.; Sando, S.; Saito, I. *Nat. Biotechnol.* **2001**, *19*, 51−55.
(39) Milner, C. M.; Campbell, R. D. *Immunogenetics* **1990**, *32*, 242−251.

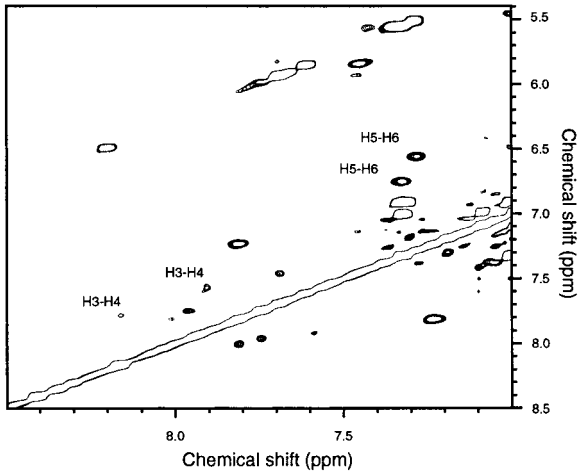

Figure 2. 2D-TOCSY spectrum for the aromatic region of the **2**−**GG1** complex.

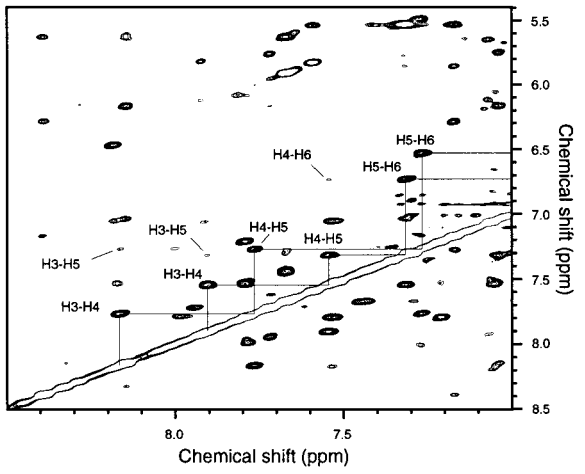

Figure 3. 2D-NOESY spectrum for the aromatic region of the **2**−**GG1** complex.

spectroscopic and thermodynamic analysis for the binding of **2** to G−G mismatch-containing DNAs. All the data described here showed that the cooperative binding of two naphthyridines to a G−G mismatch through the hydrogen bonding within the DNA π-stack is the basis for the formation of stable complexes between the drugs and mismatches.

Results and Discussion

Structural Analysis of the 2−G−G Mismatch Complex by NMR. To know the mode of the binding of naphthyridine dimer to a G−G mismatch, we have measured ^{1}H and ^{31}P NMR of the complex produced from **2** and self-complementary 9-mer duplex d(CATCGGATG)$_2$ (**GG1**) containing a G−G mismatch in the middle of the sequence.[36] The central domain of d(CGG)/(CGG) in the sequence is the site with the highest affinity for **2** binding as we previously determined by DNase I footprint titration.[38] We first focused our attention on the aromatic hydrogens of **2** in the complex. The 2D-TOCSY spectrum for the aromatic regions of the **2**−**GG1** complex was shown in Figure 2. Because two naphthyridine rings of **2** are symmetric to each other, four aromatic hydrogens corresponding to H3, H4, H5, and H6 were observed in CD_3OD at 8.28, 8.11, 8.09, and 7.33 ppm, respectively. In contrast, the aromatic hydrogens of two naphthyridines in the **2**−**GG1** complex were separately observed, showing that two naphthyridines are no longer symmetric to each other in the complex. Thus, two sets of cross-peaks for H5−H6 and H3−H4 were observed in the 2D-TOCSY spectrum of the **2**−**GG1** complex. Although signal intensities of H3−H4 cross-peaks were rather weak compared to those for H5−H6, distinct cross-peaks of H3−H4 in addition to those of H4−H5 and H5−H6 were observed in the 2D-NOESY spectrum (Figure 3). Each H6 signal of two naphthyridines in the **2**−**GG1** complex observed at 6.53 and 6.73 ppm was unambiguously assigned on the basis of a correlation with C7-methyl hydrogens observed at 2.37 and 1.75 ppm, respectively. The chemical shifts of all the eight hydrogens of two naphthyridines and C7-methyl hydrogens were summarized in Table 1. As clearly seen from the table, all signals showed substantial upfield shifts in the **2**−**GG1** complex compared to those in a free state of **2**. The upfield shifts of naphthyridine hydrogens are attributable to the ring-current effects from the aromatic rings, suggesting that both naphthyridine rings of **2** intercalated into DNA base pairs in the complex. The formation of hydrogen bonds between **2** and **GG1** is also suggested by a marked change

Table 1. Chemical Shifts (ppm) of Aromatic Hydrogens of Naphthyridine in **2** and **2**−**GG1** Complex

	H3	H4	H5	H6	7-Me
2[a]	8.28	8.11	8.09	7.33	2.67
2-GG1[b,c]	8.16	7.77	7.27	6.53	2.37
	7.91	7.54	7.32	6.73	1.75

[a] In CD_3OD. [b] In D_2O. [c] Two sets of signals were observed.

C1 A2 T3 C4 G5 ND5' G6 A7 T8 G9

G1 T2 A3 G4 ND5 G5' C6 T7 A8 C9

Figure 4. Conventional numbering of the nucleotide bases in the **2**−**GG1** complex.

of exchangeable protons in ^{1}H NMR in terms of the chemical shifts and the thermal profile of the signals (Figure S1).

To identify the intermolecular interactions, the exchangeable protons involved in the hydrogen bonding of **2** and **GG1** were identified using 2D-NOESY experiments. A conventional numbering of the nucleotide bases in the **2**−**GG1** complex for the NMR assignments was shown in Figure 4. The chemical shifts of the imino protons for G1, T2, T3, and G4 in a free state of **GG1** were reported as 12.8, 13.7, 13.6, and 12.6 ppm, respectively.[36] The imino protons of T2 (T2NH), T3 (T3NH), and G4 (G4NH) in the **2**−**GG1** complex were assigned at 13.4, 12.6, and 12.0 ppm, respectively, by observing distinct cross-peaks of T2NH with T3NH and T3NH with G4NH (Figure 5c). The signal at 12.0 ppm showed a correlation with two different imino protons at 11.75 and 11.65 ppm. A correlation between the signal at 11.65 ppm and T7NH, which is identical to T3NH in the chemical shift, identifies the imino proton as G6NH. The signal at 11.75 ppm is likely an imino proton of one of the guanines (G5 or G5′) bound to naphthyridine. These assignments of the imino protons were supported by the correlations between the imino protons of T2, T3, and G4 and an aromatic hydrogen at the C2 position of adenines A2 (A2CH) and A3 (A3CH) (Figure 5b). Thus, A2CH showed strong correlations with T2NH and T3NH, whereas A3CH correlated to all the imino protons of T2, T3, and G4. Because of fast exchange with water protons at both terminuses (G1NH and G9NH), these imino protons were not observed at 17 °C. Similarly, signal intensities for neighboring imino protons at T2NH (T8NH is overlapped) decreased with the temperature change over 37 °C (Figure S1).

A strong correlation between the signals at 12.0 and 9.00 ppm was particularly suggestive for the signal assignment, because the proton at 9.00 ppm had a correlation to the methyl

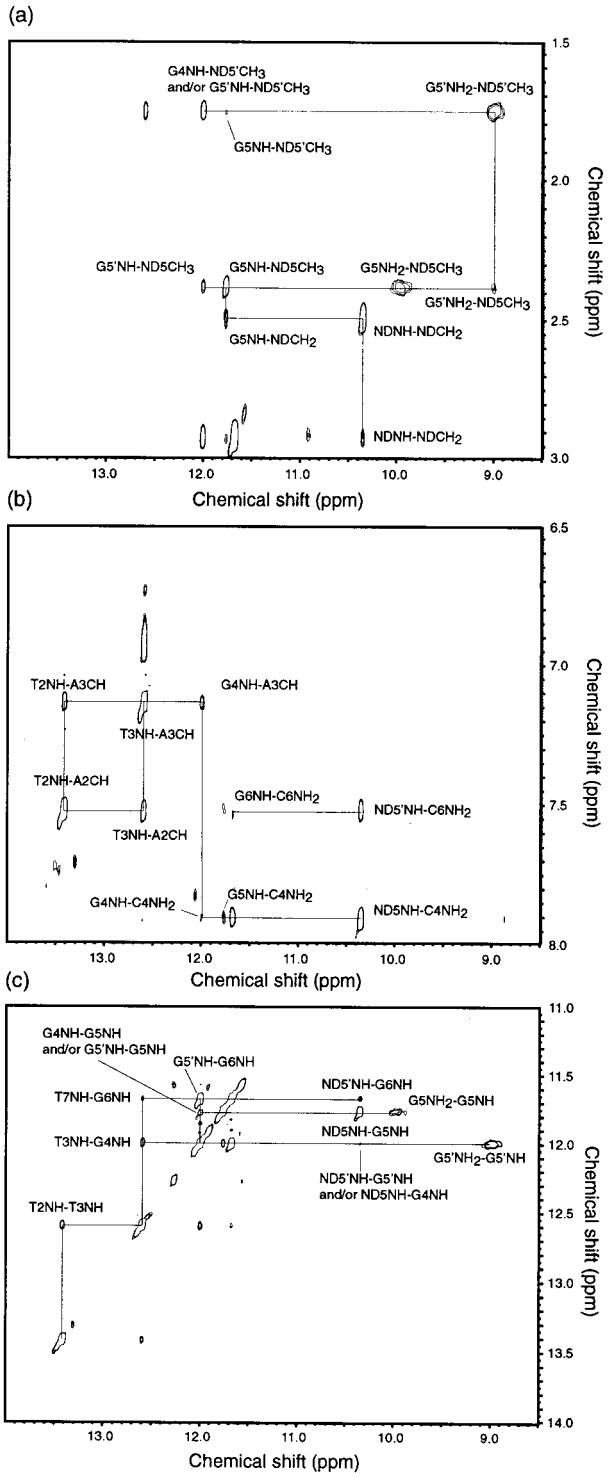

Figure 5. 2D-NOESY spectrum of the **2**−**GG1** complex involving the exchangeable protons.

hydrogens at 1.75 ppm in one of two naphthyridines (Figure 5a). The other methyl hydrogens were observed at 2.37 ppm and strongly correlated to the signal at 9.95 ppm. On the basis of a putative hydrogen-bonded guanine and 2-aminonaphthyridine pair, the signals observed at 9.95 and 9.00 ppm were assigned as the hydrogens of the amino group at the C2 position of the guanines ($G5NH_2$ and $G5'NH_2$) bound to naphthyridine. The two cross-peaks with a strong intensity were assigned to the correlations between an imino proton and an amino proton of the guanine bound to naphthyridine. Thus, two signals at 11.75 and 12.0 ppm were assigned as imino protons of G5 (G5NH) and G5′ (G5′NH), respectively. The imino proton of G5′ was overlapped by the signal of G4NH. Accordingly, the methyl group observed at 2.37 ppm was attached to the naphthyridine bound to G5 (ND5), whereas the methyl group of the other naphthyridine bound to G5′ (ND5′) appeared at 1.75 ppm. A very significant cross-peak between the methyl hydrogen of ND5 ($ND5CH_3$) and the amino hydrogen of G5′ ($G5'NH_2$) suggests a stacking of the hydrogen-bonded pairs of ND5−G5 and G5′−ND5.

The remaining signal at 10.35 ppm was assigned as the two amide protons of **2** (ND5NH and ND5′NH) bound to the carbonyl oxygens of G5 and G5′, on the basis of the correlations to the methylene hydrogens in the linker connecting two naphthyridines. Characteristic correlations to NDNH are observed for the signals at 7.53 and 7.90 ppm, which were assigned as the amino protons of C6 ($C6NH_2$) and C4 ($C4NH_2$), respectively. These assignments were supported by the correlations of G5NH−$C4NH_2$, G4NH−$C4NH_2$, and G6NH−$C6NH_2$ (Figure 5b). The correlations of ND5NH to G5NH and ND5′NH to G5′NH were also observed, although the two correlations were very much different in their intensities. NOE correlations observed for the **2**−**GG1** complex are consistent with the proposed structure of the complex, where each one of two naphthyridines binds to a guanine in the G−G mismatch and the naphthyridine−guanine pairs are stacked with each other. The observed NOEs were illustrated on the proposed chemical structure of the **2**−**GG1** complex (Figure 6). A marked highfield shift of $ND5'CH_3$ (1.75 ppm) compared to the shift of $ND5CH_3$ (2.37 ppm) suggests that $ND5CH_3$ extrudes into a minor groove, whereas $ND5'CH_3$ is probably stacked with the neighboring G−ND5 and/or G−C base pair and more strongly affected by the ring-current shielding effects. This asymmetry regarding the position of two naphthyridines in the complex reflects on an appearance of the NOE cross-peak for $ND5CH_3$−$G5'NH_2$ and the disappearance of a $ND5'CH_3$−$G5NH_2$ cross-peak. The tetrahedral structure of the basic amino nitrogen of the linker and insufficient linker length between two naphthyridines are highly likely the reasons for the asymmetric location of two naphthyridine−guanine pairs in the **2**−**GG1** complex.

^{31}P NMR spectra of **GG1** and the **2**−**GG1** complex were measured at 17 and 37 °C (Figure 7). The broad signals of **GG1** were observed between −2.7 and −2.2 ppm at 37 °C. The narrow distribution of ^{31}P chemical shifts (i.e., 0.5 ppm) indicates that dihedral angles of phosphate backbones are those in B- and A-type DNA structures at 37 °C. As the temperature decreased to 17 °C, the signals became more discrete and sharp in shape. This observation correlates well to the melting of a duplex form of **GG1** to a single strand, because the melting temperature (T_m) of **GG1** was reported to be 35 °C.[36] In contrast, the ^{31}P signals of the **2**−**GG1** complex shifted upfield by ∼1 ppm compared to those of free **GG1** and were less sensitive to a temperature change because of the increased T_m of the duplex upon complex formation. Because ^{31}P chemical shifts in nucleic acids provide a probe of the conformation of a phosphate ester,[18,40] wider distribution of ^{31}P signals in the complex compared to its free state may imply conformational changes of a phosphate backbone upon complex formation.

Conformational Change of a G−G Mismatch-Containing Duplex upon 2 Binding. The NMR spectra of the **2**−**GG1** complex showed that both naphthyridine rings intercalated in DNA base pairs. These observations implied that the structure of a mismatched site in **GG1** would be significantly changed

(40) Roongta, V. A.; Jones, C. R.; Gorenstein, D. G. *Biochemistry* **1990**, *29*, 5245−5258.

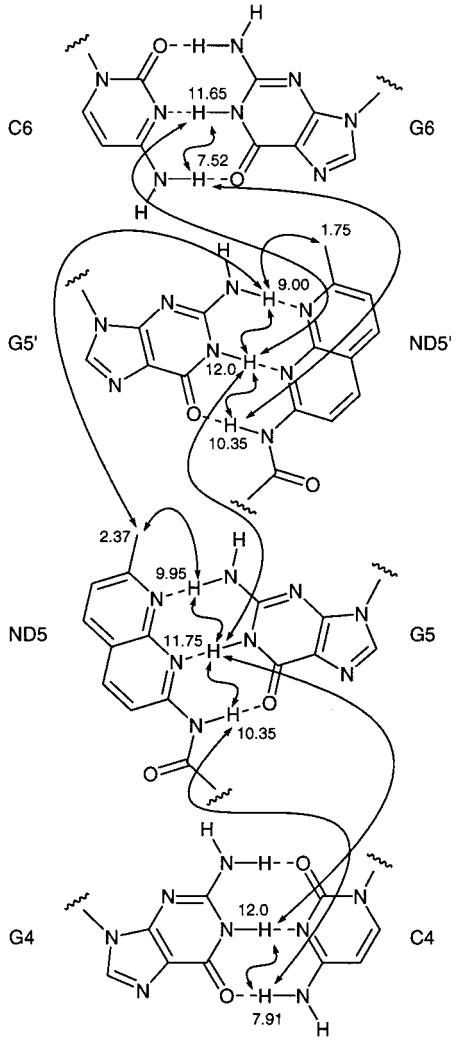

Figure 6. Illustration of chemical shifts of protons and NOEs observed for the **2**−**GG1** complex.

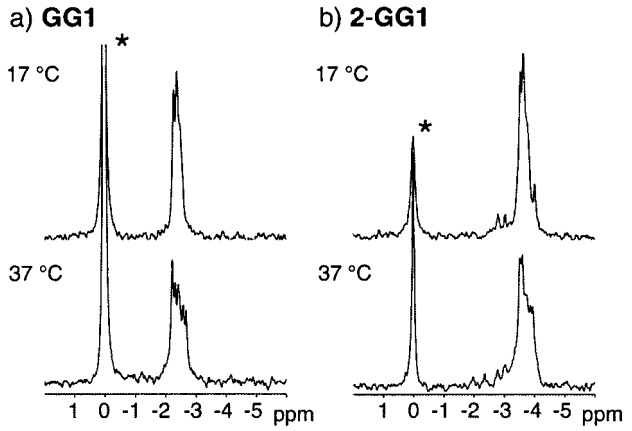

Figure 7. ^{31}P NMR spectra of (a) **GG1** and (b) **2**−**GG1** complex at 17 and 37 °C. Signals shown with an asterisk are the internal standard.

upon complex formation. CD spectra of short 11-mer duplexes d(CTA ACG GAA TG)/d(CAT TCX GTT AG) containing G−G (**GG2**: X = G) and G−A (**GA1**: X = A) mismatches were measured in the presence and absence of **2** (Figure 8). While CD spectra of **GG2** are quite similar to those of **GA1** and the fully matched duplex (X = C, data not shown), addition of 2 mol equiv of **2** into **GG2** induced a dramatic change of the spectra. The positive maximum at 270 nm increased the intensity by 2-fold, and negative bands at 250 nm of **GG2**

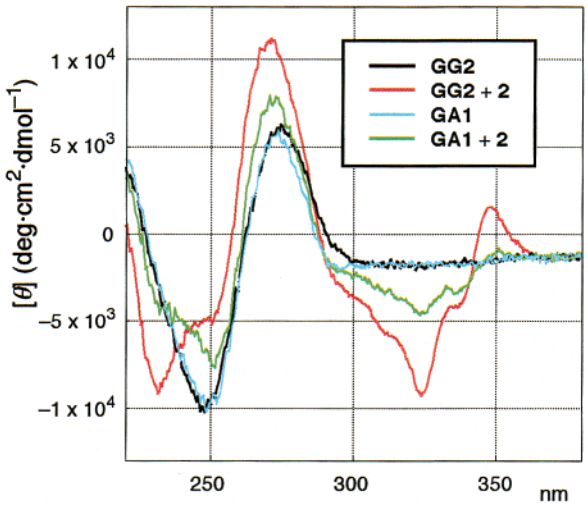

Figure 8. CD spectra of DNA duplexes d(CTA ACG GAA TG)/d(CAT TCX GTT AG) containing G−G (**GG2**: X = G) and G−A (**GA1**: X = A) mismatches in the absence and presence of **2** (9.1 μM). CD spectra of duplexes (100 μM base concentration) were measured in 10 mM sodium cacodylate buffer (pH 7.0) and 100 mM NaCl at 25 °C.

shifted to 230 nm in the **2**−**GG2** complex. Intense induced CD was also observed in the region from 300 to 360 nm, showing that naphthyridine rings are located within a chiral environment produced by a DNA double helix. Similar induced CD bands but with much weaker intensity were detected for the **2**−**GA1** complex. We have reported that the binding of **2** to the G−G mismatch in the d(CGG)/d(CGG) is about 360-fold stronger than that to the G−A mismatch in d(CGG)/d(CAG).[38] The spectral change induced by the addition of **2** is much more significant for **GG2** than for **GA1**, showing a good correlation between the CD spectral change and the efficiency of **2** binding to the mismatched site. These experiments clearly showed that binding of **2** to a G−G mismatch accompanied a significant conformational change.

Thermodynamics for the Formation of the 2−**GG2 Complex.** We have analyzed energetics and stoichiometry of the interaction between **2** and **GG2** by isothermal titration calorimetry (ITC).[41,42] In the experiments, the calorimeter cell was filled with the solution of **GG2**, and the solution of **2** was injected. Evolution of heat upon injection of **2** was measured as the power (μcal s^{-1}) that is required to maintain a zero temperature difference between the sample and the reference cell. Each injection of **2** into the solution containing **GG2** produced a large exothermic heat of reaction, whereas the dilution heat produced by adding **2** into buffer was small and negligible (Figure 9). Molar heat values obtained by integration of the data were plotted as a function of the molar ratio between **2** and **GG2** ([**2**]/[**GG2**]) (Figure 9, inset). From the best fit for the binding isotherm using a single site model, thermodynamic parameters were obtained. An apparent association constant (K_a) for the binding of **2** to **GG2** was 0.9×10^7 M^{-1}, which is consistent with K_a of 1.9×10^7 M^{-1} (K_d of 53 nM) obtained by DNase I footprint titration within experimental variability.[38] The stoichiometry (n) for the binding was 1.2, suggesting a 1:1 binding. The free energy change at 25 °C by the formation of the **2**−**GG2** complex was -9.5 ± 0.3 kcal/mol, which consisted of an enthalpy gain of -36.5 ± 0.4 kcal/mol and an entropy

(41) Haq, I.; Trent, J. O.; Chowdhry, B. Z.; Jenkins, T. C. *J. Am. Chem. Soc.* **1999**, *121*, 1768−1779.
(42) Ren, J.; Jenkins, T. C.; Chaires, J. B. *Biochemistry* **2000**, *39*, 8439−8447.

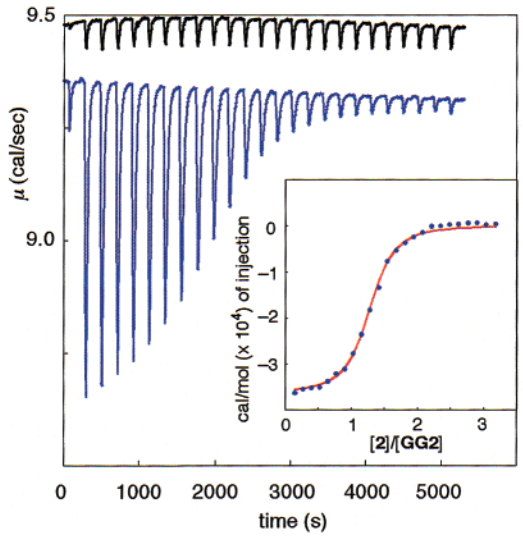

Figure 9. Isothermal titration carlorimetry (ITC) for the binding of **2** to **GG2** at 25 °C. Titration was conducted by adding 10 μL of **2** (70 μM) every 3 min into a buffer solution (10 mM sodium cacodylate pH 7.0, 100 mM NaCl) containing G−G mismatch DNA **GG2** (4 μM) (blue line) or buffer alone (black line). Inset: Molar heat values plotted as a function of the [**2**]/[**GG2**] molar ratio. The solid red line represents the best fit binding isotherm. The data were fitted using a single site model.

loss of 27.0 ± 0.7 kcal/mol. These data showed enthalpy-driven binding of **2** to a G−G mismatch.

Synthesis of Probe Molecules 3 and 4. Having confirmed the intercalation of two naphthyridines of **2** into the DNA π-stack and the hydrogen bonding between naphthyridine and guanine, we then examined the effect of the structural modification of drugs on the efficiency of the binding by using two probe molecules, **3** and **4**. In naphthyridine dimer **3**, the secondary amino group in the linker of **2** connecting two naphthyridine rings was converted to a tertiary amide. To keep the magnitude of the positive charge the same between **2** and **3**, a primary amino group was additionally incorporated into the linker. The other probe molecule **4** is the 2-aminoquinoline−naphthyridine hybrid, where one of two 2-aminonaphthyridines in **2** was replaced with 2-aminoquinoline. Synthetic schemes for **2**, **3**, and **4** were shown in Scheme 1. Methanolysis of commercially available 3-[(2-cyanoethyl)amino]propanenitrile gave dimethyl ester **5**. Reaction of **5** with di-*tert*-butyl dicarbonate afforded **6** in 83% yield. Hydrolysis of **6** with aqueous sodium hydroxide followed by the reaction with *N*-hydroxysuccinimide in the presence of 1-(3-dimethylaminopropyl)-3-ethylcarbodiimide hydrochloride (EDCI) gave activated diester **7** in 85%. Condensation of **7** with 2-amino-7-methyl-1,8-naphthyridine afforded Boc-protected dimeric naphthyridine **8** in 46%, which was hydrolyzed for deprotection to give dimeric naphthyridine **2**. Coupling of **2** with pentafluorophenyl *N*-Boc-3-aminopropanoate followed by acid treatment produced **3** in 77%. Bispentafluorophenoxy ester **10** was used instead of **7** for the synthesis of naphthyridine−aminoquinoline hybrid **4** (Scheme 2). Conversion of **5** to **10** was achieved in three steps in 57% overall yield. Subsequent coupling of **10** with 1 equiv of 2-amino-7-methylnaphthyridine produced monopentafluoroester **11** in 90%. A second coupling of **11** with 2-aminoquinoline proceeded rather sluggishly to give protected naphthyridine−aminoquinoline hybrid **12** in 34% yield, which was converted to **4** under acidic conditions.

Effects of the Drug Structure on the Mismatch Binding. The efficiency of the drug binding to **GG2** containing a G−G mismatch was examined by the difference in T_m (ΔT_m) between the presence and absence of drugs (Table 2). ΔT_m increases as the affinity of drug to a G−G mismatch increases. All drugs **1**−**4** did not stabilize fully matched duplex **GC1**, whereas the degree of the stabilization of **GG2** was varied between the drugs. In marked contrast to a large ΔT_m of 16.4 °C upon **2** binding to **GG2**, naphthyridine monomer **1** only weakly stabilized **GG2**, showing a ΔT_m of 1.8 °C under the same conditions. Duplex stabilization by dimeric naphthyridine was highly sensitive to the structure of the linker by comparing ΔT_m values obtained in the presence of **2** and **3**. A transformation of a secondary amine in the linker of **2** to a tertiary amide in **3** resulted in a decrease of ΔT_m by 6.2 °C. Acylation of the amines changes

Scheme 1[a]

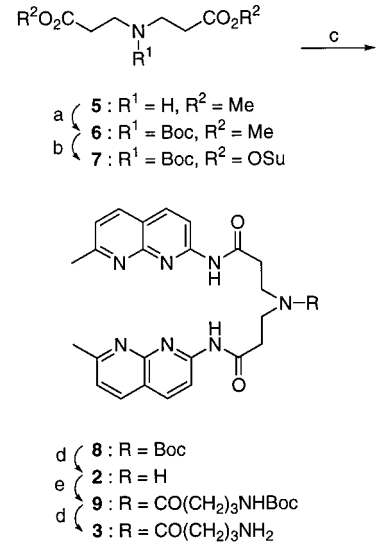

[a] Reagents: (a) Boc_2O, $CHCl_3$, 83%; (b) (i) aq NaOH, THF; (ii) *N*−hydroxysuccinimide, EDCI, DMF, 85%; (c) 2-amino-7-methyl-1,8-naphthyridine, $CHCl_3$, 46%; (d) HCl, AcOEt, $CHCl_3$, quantitative; (e) pentafluorophenyl *N*−Boc-3-aminopropanoate, diisopropylethylamine, DMF, 77%.

Scheme 2[a]

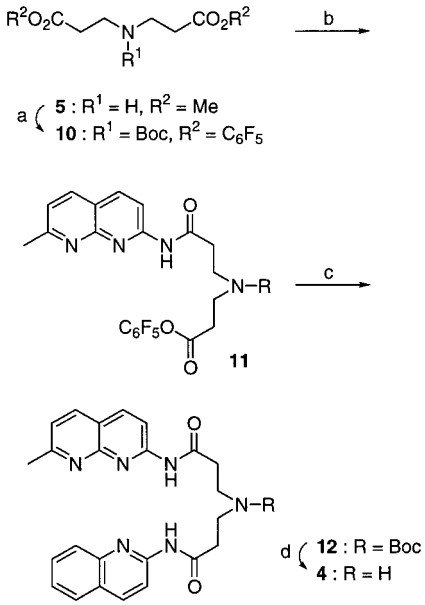

[a] Reagents: (a) (i) Boc_2O, $CHCl_3$; (ii) aq NaOH, THF; (ii) pentafluorophenol, EDCI, DMF, 57%; (b) 2-amino-7-methyl-1,8-naphthyridine, DMF, 90%; (c) 2-aminoquinoline, DMF, 34%; (d) HCl, AcOEt, $CHCl_3$, quantitative.

Table 2. Difference of Melting Temperature (ΔT_m) of G−G Mismatch-Containing Duplexes in the Presence and Absence of Drug[a,b]

5′-CTAAC**G**GAATG-3′ 3′-GATTG**X**CTTAC-5′	drug[c]			
	1	**2**	**3**	**4**
GG2: X = G	1.8	16.4	10.2	2.4
GC1: X = C	−0.3	−0.3	−0.2	−0.7

[a] The UV melting curve was measured at a total base concentration of 100 μM in 10 mM sodium cacodylate buffer (pH 7.0) containing 0.1 M NaCl. ΔT_m is the difference in T_m of the duplex obtained in the presence and absence of drug. T_m values of G−G mismatched and fully matched duplexes were 25.8 and 42.5 °C, respectively. [b] Mismatched bases are shown in boldface. [c] Concentration of drug **1** was 18.2 μM, whereas those of **2**, **3**, and **4** were 9.1 μM.

the structure from tetrahedral to trigonal planar in amide, where three atoms directly attached to the nitrogen are located on the same plane. Therefore, a weaker stabilization of **GG2** by **3** is most likely due to the increase of the energy necessary for a conformational change from a free to bound state of **3** compared to the energy required for **2**. Only a small ΔT_m of 2.4 °C was observed for **GG2** in the presence of naphthyridine−aminoquinoline hybrid **4**. We previously observed almost negligible stabilization of DNA containing a G-bulge by a 2-aminoquinoline derivative.[33] This was rationalized by a steric repulsion between C8−H of 2-aminoquinoline and N^2−H of G in a postulated 2-aminoquinoline−G hydrogen bonded pair. The stabilization of **GG2** was much stronger for **2** and **3**, containing two naphthyridine moieties in one molecule, than **4**. These observations strongly suggested that the binding of two naphthyridines to each G in the G−G mismatch is essential for the strong stabilization of the mismatch. Only a weak stabilization of **GG2** by **1** emphasized a significance of the covalent connection of two naphthyridines. The importance of three hydrogen bonds between **2** and guanine in the **2**−**GG1** complex for the strong duplex stabilization is also suggested by using oligomers containing inosine (I)−inosine and guanine−inosine mismatches. Melting temperatures of d(CTA ACX GAA TG)/d(CAT TCI GTT AG) containing a I−I mismatch (X = I) and a G−I mismatch (X = G) increased only 10.4 and 12.8 °C, respectively, in the presence of **2**, substantially lower than the increase of 16.4 °C for the G−G mismatch. Although a replacement of guanine by inosine affects not only the hydrogen bonding but also the stacking interactions, it is estimated that three hydrogen bonds in each naphthyridine−guanine pair strongly contribute to the stabilization of a G−G mismatch-containing duplex.

Implication for the Design of Mismatch Binding Molecules. The binding of dimeric naphthyridine **2** to G−G mismatch was examined by NMR and CD spectra with respect to the complex structure, and by ITC regarding the thermodynamics. All the data obtained by these analyses showed that **2** and G−G mismatches form a stable complex with 1:1 stoichiometry, where each one of two naphthyridines of **2** binds to a guanine and the two naphthyridine−guanine pairs are stacked with each other in the duplex. The structure of the linker connecting two naphthyridines was very sensitive to the binding, as clearly shown by the comparison of ΔT_m obtained for **2** and **3**. Furthermore, a loss of full complementarity of the hydrogen bonding groups to those of a mismatched base considerably decreases the affinity to the mismatch. The marked difference between **1** and **2** regarding the efficiency for the binding to a G−G mismatch strongly suggested that a cooperative binding of two naphthyridines to a G−G mismatch is essential for the formation of the stable complex. In addition to these factors, the sequence flanking the G−G mismatch has significant effects for the stabilization of the mismatch by **2** as we reported earlier.[28] The sequence dependent stabilization of the G−G mismatch by **2** suggests that the stacking of the naphthyridine−guanine pair by the flanking base pairs plays an important role for the stabilization of the complex. For the molecular design of the drugs targeting G−A and G−T mismatches, a hybrid drug consisting of naphthyridine and a planar molecule with hydrogen bonding groups fully complementary to A and T would be potentially attractive.

Experimental Section

Methyl 3-((2-(Methoxycarbonyl)ethyl)amino)propanoate (5). A solution of acetyl chloride (14.9 g, 0.19 mol) in MeOH (70 mL) was heated under reflux for 5 min. To the solution was added 3,3′-iminobis(propionitrile) (5.0 g, 0.04 mol), and the mixture was heated under reflux for 8 h. Additional acetyl chloride (5.5 g, 0.07 mol) was added, and the mixture was heated under reflux for an additional 3 h. The reaction mixture was left at room temperature overnight and filtered, and the filtrate was evaporated in vacuo to give hydrochloride of **5** (8.1 g, 88%) as a white granular solid: ^{1}H NMR (D_2O, 400 MHz) δ 3.60 (s, 6 H), 3.24 (t, 4 H, J = 6.4 Hz), 2.73 (t, 4 H, J = 6.4 Hz); ^{13}C NMR (D_2O, 100 MHz) δ 172.9, 52.7, 43.1, 30.0; FABMS (NBA), *m*/*e* 189 [(M + H)$^+$]; HR-FABMS calcd for $C_8H_{15}O_4N$ [(M + H)$^+$], 189.1000; found, 189.1006.

Methyl 3-((*tert*-Butoxy)-*N*-(2-(methoxycarbonyl)ethyl)carbonylamino)propanoate(6). To a suspension of the hydrochloride of **5** (1.0 g, 4.4 mmol) in $CHCl_3$ (30 mL) was added triethylamine (0.73 g, 7.2 mmol) at 0 °C. After stirring for 1 h, the reaction mixture was filtered, and the filtrate was evaporated in vacuo to give free 3,3′-iminobis(methyl propionate) as a white solid. To the solution of this material in dry $CHCl_3$ (6 mL) was added di-*tert*-butyl dicarbonate (1.06 g, 4.9 mmol) slowly at 0 °C, and the mixture was stirred overnight at room temperature. The solution was washed successively with saturated aqueous $KHSO_4$, saturated aqueous $NaHCO_3$, and saturated aqueous NaCl and dried over $MgSO_4$. Solvent was evaporated to give **6** (1.06 g, 83%) as an oil: ^{1}H NMR ($CDCl_3$, 400 MHz) δ 3.64 (s, 6 H), 3.46 (m, 4 H), 2.53 (m, 4 H), 1.41 (s, 9 H); ^{13}C NMR ($CDCl_3$, 100 MHz, 50 °C) δ 172.1, 154.9, 79.9, 51.5, 44.0, 33.5, 28.2; EIMS, *m*/*e* (%) 289 (M$^+$) (3), 233 (20), 202 (45), 174 (25), 57 (100); HRMS calcd for $C_{13}H_{23}NO_6$ (M$^+$), 289.1525; found, 289.1515.

2,5-Dioxopyrrolidinyl 3-((*tert*-Butoxy)-*N*-(2-((2,5-dioxopyrrolidinyl)oxycarbonyl)ethyl)carbonylamino)propanoate (7). To a stirred solution of **6** (283 mg, 0.98 mmol) in THF (1.25 mL) was added 2 N aqueous NaOH solution (1.25 mL, 3 mmol), and the mixture was vigorously stirred at room temperature for 20 h. MeOH (1.25 mL) was added, the reaction mixture was neutralized to pH 7 with Amberlite IR-120 (H$^+$ form) ion-exchange resin, and the whole mixture was stirred overnight. The mixture was readjusted to pH 3.5 with the resin and filtered, and the solvent was evaporated to give *N*-(*tert*-butoxycarbonyl)-imino-3,3′-bis(propionic acid) as a white solid. To the solution of acid in dry DMF (5 mL) were added *N*-hydroxysuccinimide (282 mg, 2.5 mmol) and 1-(3-dimethylaminopropyl)-3-ethylcarbodiimide hydrochloride (470 mg, 2.5 mmol). The mixture was stirred for 48 h at room temperature. The solvent was evaporated, and the crude product was suspended in $CHCl_3$. The organic layer was washed successively with H_2O, saturated aqueous $NaHCO_3$, and saturated aqueous NH_4Cl and dried over $MgSO_4$. The solvent was evaporated to give **7** (358 mg, 85%) as a white solid: ^{1}H NMR ($CDCl_3$, 400 MHz) δ 3.59 (m, 4 H), 2.89 (m, 2 H), 2.83 (m, 2 H), 2.79 (s, 8 H), 1.43 (s, 9 H); ^{13}C NMR ($CDCl_3$, 100 MHz) δ 168.9, 167.3, 154.8, 80.9, 44.6, 36.5, 30.8, 28.3, 25.6; FABMS (NBA), *m*/*e* 456 [(M + H)$^+$]; HR-FABMS calcd for $C_{19}H_{26}O_{10}N_3$ [(M + H)$^+$], 456.1616; found, 456.1591.

3-((*tert*-Butoxy)-*N*-(2-(*N*-(7-methylpyridino[3,2-e]pyridin-2-yl)-carbamoyl)ethyl)carbonylamino)-*N*-(7-methylpyridino[3,2-e]pyridin-2-yl)propanoate (8). To a solution of **7** (313 mg, 0.74 mmol) in dry $CHCl_3$ (30 mL) was added 2-amino-7-methyl-1,8-naphthyridine (294 mg, 1.9 mmol), and the mixture was stirred at room temperature for 48 h. The mixture was filtered, the filtrate was evaporated to dryness, and the crude residue was purified by silica gel column chromatography to give **8** (185 mg, 46%) as a pale yellow solid: ^{1}H NMR ($CDCl_3$, 400 MHz) δ 8.78 (br, 2 H), 8.45 (d, 2 H, J = 8.8 Hz), 8.13 (d, 2 H, J =

8.8 Hz), 7.98 (d, 2 H, $J = 8.4$ Hz), 7.25 (d, 2 H, $J = 8.4$ Hz), 3.65 (t, 4 H, $J = 6.8$ Hz), 2.77 (t, 4 H), 2.74 (s, 6 H), 1.37 (s, 9 H); ^{13}C NMR ($CDCl_3$, 100 MHz) δ 171.2, 163.2, 155.4, 154.4, 153.9, 139.4, 121.8, 118.8, 115.0, 80.5, 44.8, 37.7, 28.8, 26.0; FABMS (NBA), *m/e* 544 [$(M + H)^+$]; HR-FABMS calcd for $C_{29}H_{34}O_4N_7$ [$(M + H)^+$], 544.2645; found, 544.2670.

***N*-(7-Methylpyridino[3,2-e]pyridin-2-yl)-3-((2-(*N*-(7-methylpyridino[3,2-e]pyridin-2-yl)carbamoyl)ethyl)amino)propanoate (2).** To a solution of **8** (50 mg, 0.09 mmol) in ethyl acetate (3 mL) was added ethyl acetate containing 4 M HCl (1.5 mL) at 0 °C, and the mixture was stirred at room temperature for 2 h. The solvent was evaporated to dryness to give the hydrochloride of **2** (quantitative yield) as a white solid. The hydrochloride of **2** was dissolved in H_2O and extracted into $CHCl_3$ by the addition of 28% aqueous ammonia solution. The organic layer was dried over $MgSO_4$, and the solvent was evaporated in vacuo to give **2** (34 mg, 84%) as a pale yellow solid: ^{1}H NMR ($CDCl_3$, 400 MHz) δ 8.39 (d, 2 H, $J = 8.8$ Hz), 8.03 (d, 2 H, $J = 8.8$ Hz), 7.93 (d, 2 H, $J = 8.0$ Hz), 7.21 (d, 2 H, $J = 8.0$ Hz), 3.10 (t, 4 H, $J = 6.0$ Hz), 2.77 (t, 4 H, $J = 6.0$ Hz), 2.72 (s, 6 H); ^{13}C NMR ($CDCl_3$, 100 MHz) δ 171.9, 163.0, 154.6, 153.7, 138.7, 136.3, 121.3, 118.4, 114.6, 44.6, 36.8, 25.5; FABMS (NBA), *m/e* 444 [$(M + H)^+$]; HR-FABMS calcd for $C_{24}H_{26}O_2N_7$ [$(M + H)^+$], 444.2146; found, 444.2148.

4-((*tert*-Butoxy)carbonylamino)-*N*,*N*-bis(2-(*N*-(7-methylpyridino-[3,2-e]pyridin-2-yl)carbamoyl)ethyl)butanamide (9). To a solution of **2** (200 mg, 0.23 mmol) dissolved in DMF (5 mL) were added pentafluorophenyl 4-(*tert*-butoxy)carbonylaminobutylate (100 mg, 0.27 mmol) and diisopropylethylamine, and the solution was stirred overnight. Solvents were evaporated, and the residue was chromatographed on a silica gel column (chloroform−methanol = 50:1) to give **9** (223 mg, 87%); ^{1}H NMR (400 MHz, $CDCl_3$) δ 10.0 (broad, 1 H), 9.54 (broad, 1 H), 8.37 (d, 2 H, $J = 8.9$ Hz), 8.06 (d, 2 H, $J = 8.8$ Hz), 7.94 (d, 1 H, $J = 8.1$ Hz), 7.91 (d, 1 H, $J = 8.3$ Hz), 7.22 (d, 1 H, $J = 8.2$ Hz), 7.18 (d, 1 H, $J = 8.1$ Hz), 5.21 (broad, 1 H), 3.76 (broad, 2 H), 3.66 (broad, 2 H), 3.08 (broad, 2 H), 2.82 (broad, 4 H), 2.69 (s, 6 H), 2.41 (t, 2 H, $J = 7.1$), 1.78 (broad, 2 H), 1.35 (s, 9 H); ^{13}C NMR (100 MHz, CDCl3) δ 173.2, 171.3, 170.2, 163.2, 163.0, 156.1, 153.5, 139.1, 139.0, 136.4, 136.3, 121.6, 121.4, 118.5, 118.4, 114.6, 78.9, 77.3, 77.2, 77.0, 76.7, 44.6, 42.1, 40.0, 36.8, 36.2, 30.2, 28.4, 25.2, 25.5, 25.3; FABMS (NBA), *m/e* (%) 629 [$(M + H)^+$] (40); HR-FABMS calcd for $C_{33}H_{41}O_4N_4F_5$, 629.3200; found, 629.3193.

4-Amino-*N*,*N*-bis(2-(*N*−(7-methylpyridino[3,2-e]pyridin-2-yl)carbamoyl)ethyl)butanamide (3). To a solution of **9** (220 mg, 0.35 mmol) in chloroform (1 mL) was added 3 N HCl in AcOEt (5 mL) at 0 °C, and the solution was stirred at room temperature for 30 min. The resulting solution was evaporated. Water and aqueous ammonia were added to the solution (pH > 7), and the resulting solution was extracted with chloroform and dried with $MgSO_4$. The solution was evaporated to give **3** (167 mg, 90%). ^{1}H NMR (400 MHz, $CDCl_3$) δ 7.76 (broad, 1 H), 7.68−7.61 (3 H), 7.54 (d, 1 H, $J = 9.0$) 7.43 (d, 1 H, $J = 8.2$), 7.00 (d, 1 H, $J = 8.2$), 6.81 (d, 1 H, $J = 8.0$), 3.63 (t, 2 H, $J = 5.9$), 3.56 (t, 2 H, $J = 6.2$), 2.95 (t, 2 H, $J = 7.5$), 2.71−2.62 (7 H), 2.40 (s, 3 H), 2.35 (s, 3 H), 1.87 (p, 2 H, $J = 7.5$); ^{13}C NMR (100 MHz, $CDCl_3$) δ 183.1, 178.0, 176.0, 174.9, 166.0, 165.8, 155.1, 154.9, 142.4, 142.2, 140.1, 124.7, 124.5, 120.8, 116.6, 116.6, 47.4, 46.3, 41.8, 38.6, 38.4, 32.7, 26.6, 25.8, 25.2; FABMS (NBA), *m/e* (%) 529 [$(M + H)^+$] (40); HR-FABMS calcd $C_{29}H_{33}N_9O_3$, 529.2676; found, 529.2694.

Pentafluorophenyl-3-((*tert*-butoxy)-*N*-(2-((pentafulorophenyl)oxycarbonyl)ethyl)carbonylamino)propanoate (10). Compound **5** was converted to *N*-(*tert*-butoxycarbonyl)iminobis(propionic acid) as described above. To a solution of *N*-(*tert*-butoxycarbonyl)iminobis-(propionic acid) (6.2 g, 24 mmol) in DMF were added pentafluorophenol (10.5 g, 57 mmol) and 1-(3-dimethylaminopropyl)-3-ethylcarbodiimide hydrochloride (10.9 g, 57 mmol). The mixture was stirred for 24 h at room temperature. The solvent was evaporated, and the crude product was suspended in $CHCl_3$. The organic layer was washed with H_2O and dried over $MgSO_4$. The solvent was evaporated in vacuo, and the crude residue was purified by silica gel column chromatography to give **9** (8.0 g, 57%) as a white solid: ^{1}H NMR ($CDCl_3$, 400 MHz) δ 3.65 (m, 4 H), 2.99 (m, 2 H), 2.93 (m, 2 H), 1.47 (s, 9 H); FABMS (NBA), *m/e* 594 [$(M + H)^+$]; HR-FABMS calcd for $C_{23}H_{18}O_6NF_{10}$ [$(M + H)^+$], 594.0973; found, 594.0971.

3-((*tert*-Butoxy)-*N*-(2-(*N*-(2-quinolyl)carbamoyl)ethyl)carbonylamino)-*N*-(7-methylpyridino[3,2-e]pyridin-2-yl)propanamide (12). To a solution of **9** (1.5 g, 2.5 mmol) in dry DMF (5 mL) was added 2-amino-7-methyl-1,8-naphthyridine (180 mg, 1.1 mmol) and diisopropylethylamine (163 mg, 1.26 mmol). The mixture was stirred at room temperature for 15 h. The solvent was evaporated to dryness, and the crude residue was purified by silica gel column chromatography to give **11** (1.29 g, 90%) as a pale yellow solid: ^{1}H NMR ($CDCl_3$, 400 MHz) δ 9.01 (br, 1 H), 8.44 (d, 1 H, $J = 8.8$ Hz), 8.12 (d, 1 H, $J = 8.8$ Hz), 7.99 (d, 1 H, $J = 8.0$ Hz), 7.26 (d, 1 H, $J = 8.0$ Hz), 3.66 (m, 4 H), 2.90 (m, 2 H), 2.74 (m, 2 H), 2.73 (s, 3 H), 1.42 (s, 9 H); FABMS (NBA), *m/e* 569 [$(M + H)^+$]; HR-FABMS calcd for $C_{26}H_{26}O_5N_4F_5$ [$(M + H)^+$], 569.1821; found, 569.1827. To a solution of **11** (587 mg, 1.0 mmol) in dry DMF (2 mL) was added 2-aminoquinoline (180 mg, 1.2 mmol) and diisopropylethylamine (160 mg, 1.2 mmol). The mixture was stirred at room temperature for 48 h. The solvent was evaporated to dryness, and the crude residue was purified by silica gel column chromatography to give **12** (187 mg, 34%) as a pale yellow solid: ^{1}H NMR ($CDCl_3$, 400 MHz) δ 8.95 (s, 1 H), 8.73 (s, 1 H), 8.44 (d, 1 H, $J = 8.8$ Hz), 8.27 (d, 1 H, $J = 8.0$ Hz), 8.12 (d, 1 H, $J = 8.8$ Hz), 8.07 (d, 1 H, $J = 8.8$ Hz), 7.95 (d, 1 H, $J = 8.0$ Hz), 7.75 (d, 1 H, $J = 8.8$ Hz), 7.71 (d, 1 H, $J = 8.0$ Hz), 7.61 (t, 1 H, $J = 7.0$ Hz), 7.40 (t, 1 H, $J = 7.0$ Hz), 7.19 (d, 1 H, $J = 8.0$ Hz), 3.64 (m, 2 H), 3.63 (m, 2 H), 2.74 (m, 2 H), 2.73 (m, 2 H), 2.72 (s, 3 H), 1.38 (s, 9 H); ^{13}C NMR ($CDCl_3$, 100 MHz) δ 170.6, 170.4, 163.2, 155.4, 154.4, 153.3, 150.8, 146.5, 139.1, 138.6, 136.5, 129.9, 127.5, 127.3, 126.9, 125.1, 121.6, 118.6, 114.4, 114.3, 80.4, 77.2, 44.7, 37.3, 30.9, 28.3, 25.5; FABMS (NBA), *m/e* 529 [$(M + H)^+$]; HR-FABMS calcd for $C_{29}H_{33}O_4N_6$ [$(M + H)^+$], 529.2561; found, 529.2565.

***N*-(7-Methylpyridino[3,2-e]pyridin-2-yl)-3-((2-(*N*-(2-quinolyl)carbamoyl)ethyl)amino)propanamide (4).** To a solution of **12** (116 mg, 0.22 mmol) in $CHCl_3$ (3 mL) was added ethyl acetate containing 4 M HCl (2 mL) at 0 °C, and the mixture was stirred at room temperature for 0.5 h. The solvent was evaporated to dryness to give hydrochloride of **4** (quantitative yield) as a white solid: ^{1}H NMR (CD_3OD, 400 MHz) δ 8.94 (d, 1 H, $J = 8.4$ Hz), 8.92 (d, 1 H, $J = 8.4$ Hz), 8.70 (d, 1 H, $J = 8.8$ Hz), 8.65 (d, 1 H, $J = 8.8$ Hz), 8.21 (d, 1 H, $J = 8.4$ Hz), 8.18 (d, 1 H, $J = 8.4$ Hz), 8.05 (t, 1 H, $J = 7.2$ Hz), 7.85 (d, 1 H, $J = 8.4$ Hz), 7.83 (t, 1 H, $J = 7.2$ Hz), 7.65 (d, 1 H, $J = 8.4$ Hz), 3.60 (t, 2 H, $J = 6.4$ Hz), 3.55 (t, 2 H, $J = 6.4$ Hz), 3.31 (t, 2 H, $J = 6.4$ Hz), 3.23 (t, 2 H, $J = 6.4$ Hz), 2.99 (s, 3 H); ^{13}C NMR (CD_3OD, 100 MHz) δ 174.5, 172.4, 161.4, 158.3, 150.6, 148.6, 147.5, 145.2, 141.5, 135.4, 134.2, 130.2, 129.5, 126.5, 123.7, 121.5, 118.8, 118.2, 114.9, 44.6, 44.0, 33.9, 33.8, 20.8; FABMS (NBA), *m/e* 429 [$(M + H)^+$]; HR-FABMS calcd for $C_{24}H_{25}O_2N_6$ [$(M + H)^+$], 429.2037; found, 429.2038.

Isothermal Titration Calorimetry (ITC). ITC titration experiments were performed on a VP MicroCalorimetry System. The experiment was conducted by adding **2** (70 μM) every 3 min into a sodium cacodylate buffer (10 mM, pH 7.0) containing NaCl (100 mM) and 11-mer G−G mismatch-containing duplex d(CTA ACG GAA TG)/d(CAT TCG GTT AG) (**GG2**) (0 or 4 μM) at 25 °C.

NMR Measurements of 2−GG1 Complex. DNA duplex **GG1** (1 mM in H_2O) both in free and complex states with **2** was pipetted into a Shigemi microtube. The NMR experiments were performed on Bruker DRX-600 and JEOL α-400 spectrometers. The total correlated spectroscopy (TOCSY) spectra were recorded with mixing time of 60 ms, and nuclear Overhauser effect spectroscopy (NOESY) spectra were recorded with mixing time of 300 ms. Total of 32 (TOCSY) and 64 (NOESY) transients were acquired with a recycle delay of 1.2 s at 17 °C. The ^{31}P NMR spectra were taken with proton decoupling sequence during acquisition time.

Acknowledgment. We thank Mr. Junji Nakamura and Mr. Yuji Hirohata of Nihon SiberHegner Co., Ltd. for ITC measurements. This research was supported in part by a grant-in-aid for scientific research on priority areas (C) "medical genome science" from the Ministry of Education, Science, Sports and Culture of Japan.

Supporting Information Available: Thermal profile of imino protons in ^{1}H NMR of **GG1** and the **2−GG1** complex (PDF). This material is available free of charge via the Internet at http://pubs.acs.org.

JA0109186